Electronic Supplementary Information (ESI)

Two-dimensional self-assemblies of azobenzene derivatives: effects of methyl substitution of azobenzene core and alkyl chain length

Yoshihiro Kikkawa,* Mayumi Nagasaki and Yasuo Norikane*

National Institute of Advanced Industrial Science and Technology (AIST), Tsukuba Central 5, 1-1-1 Higashi, Tsukuba, Ibaraki 305-8565, Japan

1. Characterization of Azobenzene derivatives

^{1}H NMR data:

AzC8: δH (400 MHz; $CDCl_3$; Me_4Si) 0.89 (6H, t, *J* = 6.7 Hz), 1.30 (16H, m), 1.48 (4H, m), 1.82 (4H, m), 4.03 (4H, t, *J* = 6.6 Hz), 6.99 (2H, d, *J* = 8.9 Hz) and 7.86 (2H, d, *J* = 8.9 Hz).

AzC9: δH (400 MHz; $CDCl_3$; Me_4Si) 0.88 (6H, t, *J* = 6.8 Hz), 1.29 (20H, m), 1.48 (4H, m), 1.81 (4H, m), 4.03 (4H, t, *J* = 6.6 Hz), 6.99 (2H, d, *J* = 8.9 Hz) and 7.86 (2H, d, *J* = 8.9 Hz).

AzC10: δH (400 MHz; $CDCl_3$; Me_4Si) 0.89 (6H, t, *J* = 6.8 Hz), 1.28 (24H, m), 1.48 (4H, m), 1.81 (4H, m), 4.03 (4H, t, *J* = 6.6 Hz), 6.99 (2H, d, *J* = 9.0 Hz) and 7.86 (2H, d, *J* = 9.0 Hz).

AzC11: δH (400 MHz; $CDCl_3$; Me_4Si) 0.88 (6H, t, *J* = 6.9 Hz), 1.27 (28H, m), 1.48 (4H, m), 1.81 (4H, m), 4.03 (4H, t, *J* = 6.6 Hz), 6.98 (2H, d, *J* = 9.0 Hz) and 7.86 (2H, d, *J* = 9.0 Hz).

AzC13: δH (400 MHz; $CDCl_3$; Me_4Si) 0.88 (6H, t, *J* = 6.8 Hz), 1.27 (36H, m), 1.47 (4H, m), 1.81 (4H, m), 4.03 (4H, t, *J* = 6.6 Hz), 6.98 (2H, d, *J* = 9.0 Hz) and 7.86 (2H, d, *J* = 9.0 Hz).

DAzC8: δH (400 MHz; $CDCl_3$; Me_4Si) 0.89 (6H, t, *J* = 6.8 Hz), 1.30 (16H, m), 1.48 (4H, m), 1.83 (4H, m), 2.29 (6H, s), 4.04 (4H, t, *J* = 6.4 Hz), 6.90 (2H, d, *J* = 9.4 Hz) and 7.72 (4H, m).

DAzC9: δH (400 MHz; $CDCl_3$; Me_4Si) 0.89 (6H, t, *J* = 6.8 Hz), 1.28 (20H, m), 1.48 (4H, m), 1.81 (4H, m), 2.29 (6H, s), 4.04 (4H, t, *J* = 6.4 Hz), 6.90 (2H, d, *J* = 9.4 Hz) and 7.73 (4H, m).

DAzC10: δH (400 MHz; $CDCl_3$; Me_4Si) 0.89 (6H, t, *J* = 6.9 Hz), 1.29 (24H, m), 1.48 (4H, m), 1.81 (4H, m), 2.29 (6H, s), 4.04 (4H, t, *J* = 6.4 Hz), 6.90 (2H, d, *J* = 9.4 Hz) and 7.73 (4H, m).

DAzC11: δH (400 MHz; $CDCl_3$; Me_4Si) 0.88 (6H, t, *J* = 6.8 Hz), 1.27 (28H, m), 1.48 (4H, m), 1.83 (4H, m), 2.29 (6H, s), 4.04 (4H, t, *J* = 6.5 Hz), 6.90 (2H, d, *J* = 9.3 Hz) and 7.72 (4H, m).

DAzC13: δH (400 MHz; $CDCl_3$; Me_4Si) 0.88 (6H, t, *J* = 6.8 Hz), 1.27 (36H, m), 1.47 (4H, m), 1.81 (4H, m), 2.29 (6H, s), 4.04 (4H, t, *J* = 6.4 Hz), 6.90 (2H, d, *J* = 9.4 Hz) and 7.73 (4H, m).

2. Additional STM images

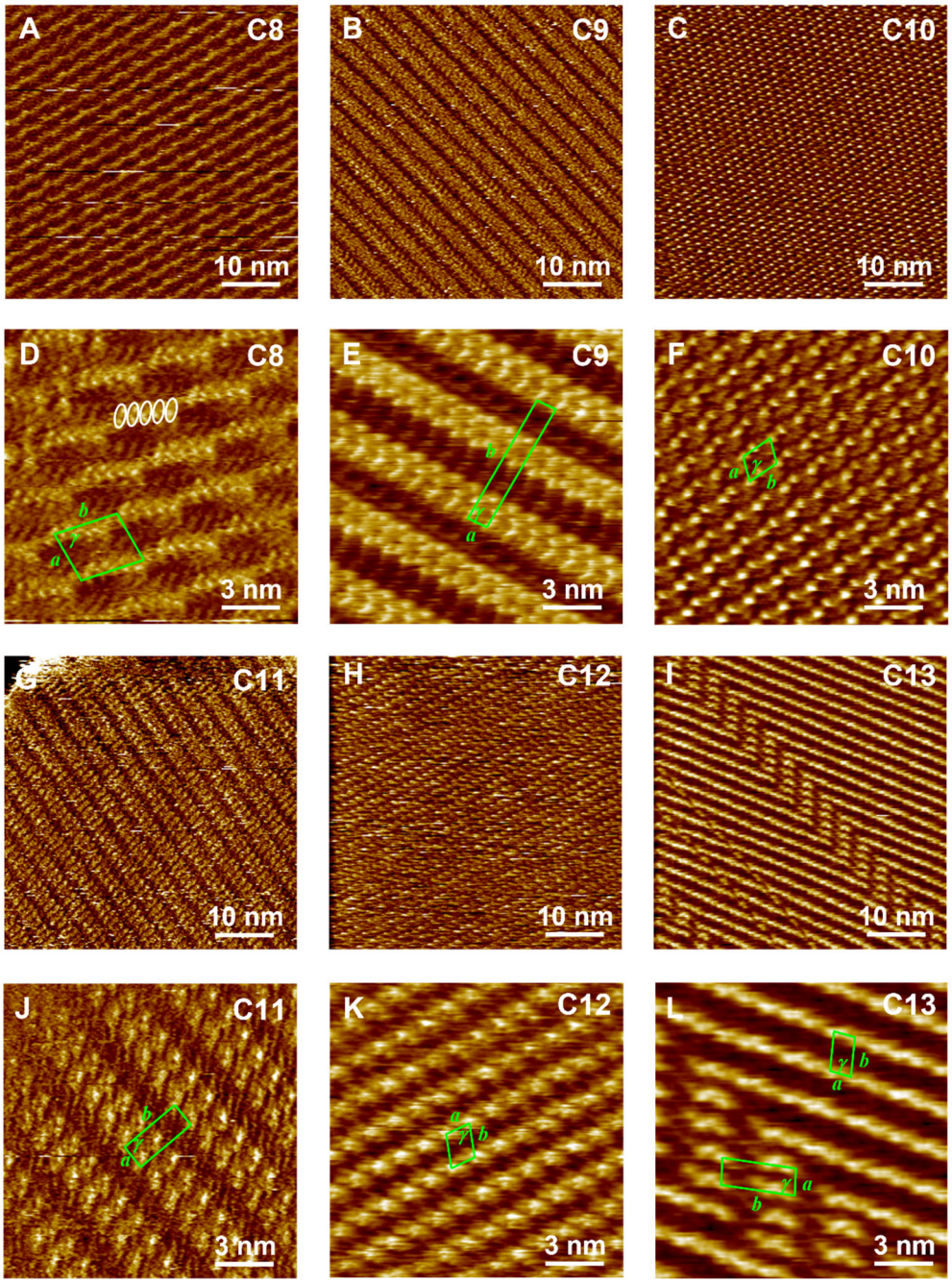

Fig. S1 Wide area (A-C, G-I) and enlarged STM images (D-F, J-L) of **Az** compounds at the HOPG/1-phenyloctane interface: (A, D) **AzC8**, (B, E) **AzC9**, (C, F) **AzC10**, (G, J) **AzC11**, (H, K) **AzC12**, (I, L) **AzC13**. In (D), five **Az** cores forming a cluster are indicated by white ovals. The 2D lattice in Table 1 is drawn in green. Tunnelling conditions: (A) I = 25 pA, V = −1013 mV; (B) I = 25 pA, V = −752 mV; (C) I = 50 pA, V = −684 mV; (D) I = 25 pA, V = −752 mV; (E) I = 50 pA, V = −850 mV; (F) I = 50 pA, V = −900 mV; (G) I = 25 pA, V = −1000 mV; (H) I = 25 pA, V = −500 mV; (I) I = 50 pA, V = −648 mV; (J) I = 25 pA, V = −1088 mV; (K) I = 25 pA, V = −500 mV; (L) I = 50 pA, V = −648 mV.

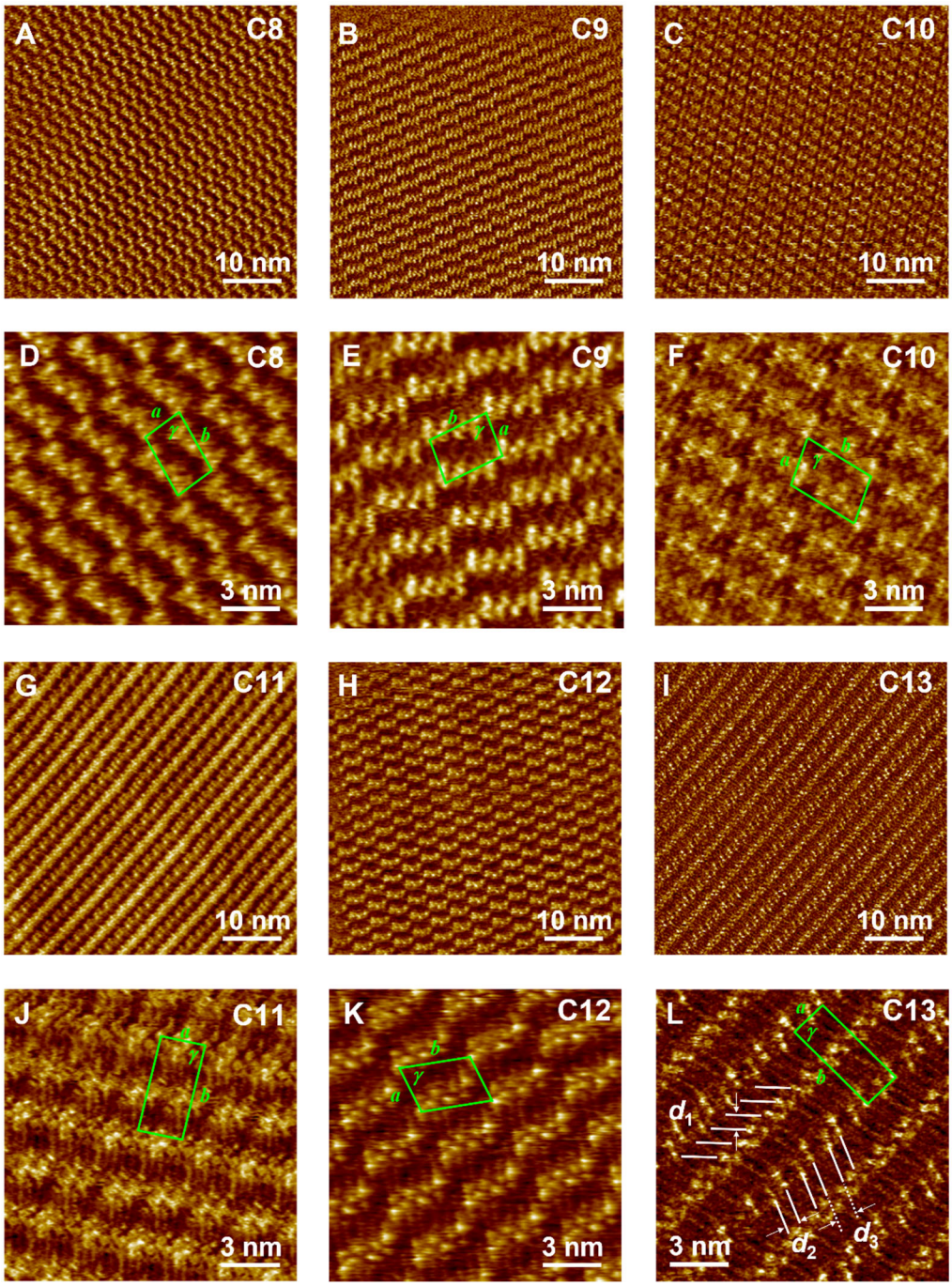

Fig. S2 Wide area (A-C, G-I) and enlarged STM images (D-F, J-L) of **MAz** compounds at the HOPG/1-phenyloctane interface: (A, D) **MAzC8**, (B, E) **MAzC9**, (C, F) **MAzC10**, (G, J) **MAzC11**, (H, K) **MAzC12**, (I, L) **MAzC13**. The 2D lattice in Table 2 is drawn in green. Tunnelling conditions: (A) I = 50 pA, V = −800 mV; (B) I = 50 pA, V = −684 mV; (C) I = 25 pA, V = −500 mV; (D) I = 50 pA, V = −800 mV; (E) I = 50 pA, V = −684 mV; (F) I = 25 pA, V = −617 mV; (G) I = 30 pA, V = −850 mV; (H) I = 25 pA, V = −292 mV; (I) I = 25 pA, V = −731 mV; (J) I = 30 pA, V = −850 mV; (K) I = 30 pA, V = −639 mV; (L) I = 25 pA, V = −731 mV.

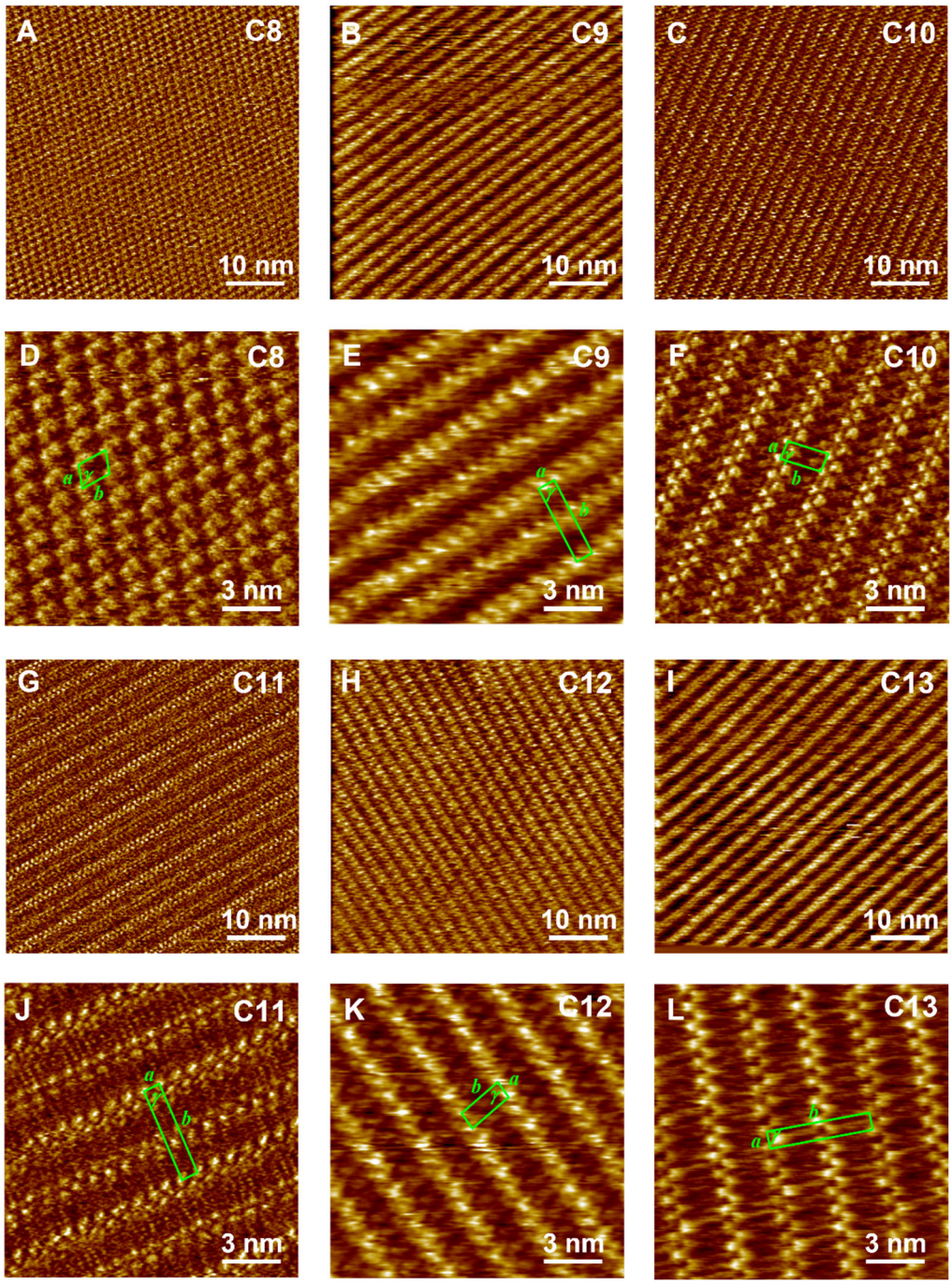

Fig. S3 Wide area (A-C, G-I) and enlarged STM images (D-F, J-L) of **DAz** compounds at the HOPG/1-phenyloctane interface: (A, D) **DAzC8**, (B, E) **DAzC9**, (C, F) **DAzC10**, (G, J) **DAzC11**, (H, K) **DAzC12**, (I, L) **DAzC13**. The 2D lattice in Table 3 is drawn in green. Tunnelling conditions: (A) I = 25 pA, V = −778 mV; (B) I = 50 pA, V = −426 mV; (C) I = 50 pA, V = −1000 mV; (D) I = 25 pA, V = −971 mV; (E) I = 50 pA, V = −321 mV; (F) I = 50 pA, V = −1000 mV; (G) I = 25 pA, V = −566 mV; (H) I = 100 pA, V = −72 mV; (I) I = 25 pA, V = −1209 mV; (J) I = 25 pA, V = −589 mV; (K) I = 150 pA, V = −403 mV; (L) I = 25 pA, V = −809 mV.

3. Angle measurements of MAz compounds

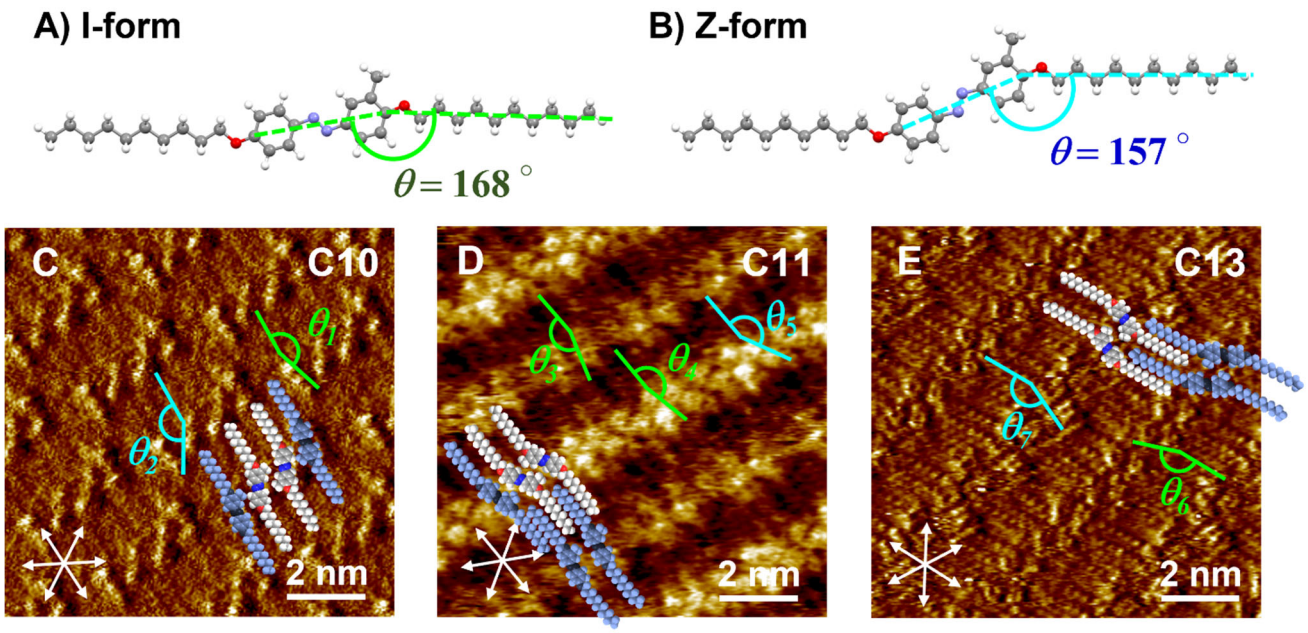

Fig. S4 Optimized geometries of **MAz** molecule with (A) I- and (B) Z-forms obtained by DFT calculations (Gaussian 16 program[S1]; B3LYP/6-311G** level[S2] with the Grimme's D3 dispersion correction[S3]). The angles between the directions of alkyl chain and core units (θ) are 168° (I-form) and 157° (Z-form). The panels (C-E) show the STM images of **MAzC10**, **MAzC11**, and **MAzC13**, respectively. Proposed molecular models are superimposed on the STM images. The θ measured from the STM images are [**MAzC10**: $\theta_1 = 169 \pm 2°$, $\theta_2 = 148 \pm 4°$], [**MAzC11**: $\theta_3 = 169 \pm 2°$, $\theta_4 = 170 \pm 2°$, $\theta_5 = 153 \pm 4°$], and [**MAzC13**: $\theta_6 = 168 \pm 2°$, $\theta_7 = 153 \pm 4°$]. The angles of θ_1, θ_3, θ_4, and θ_6 (green colour) are for the I-form molecules, whereas those of θ_2, θ_5, and θ_7 (cyan colour) indicate the values for I-form ones. Although the θ_2, θ_5, and θ_7 are a little smaller, the measured data are almost identical to the angles from DFT calculation within the error. Tunnelling conditions: (A) I = 25 pA, V = −584 mV; (B) I = 30 pA, V = −850 mV; (C) I = 100 pA, V = −750 mV.

References:

S1 M. J. Frisch, G. W. Trucks, H. B. Schlegel, G. E. Scuseria, M. A. Robb, J. R. Cheeseman, G. Scalmani, V. Barone, G. A. Petersson, H. Nakatsuji, X. Li, M. Caricato, A. V. Marenich, J. Bloino, B. G. Janesko, R. Gomperts, B. Mennucci, H. P. Hratchian, J. V. Ortiz, A. F. Izmaylov, J. L. Sonnenberg, D. Williams-Young, F. Ding, F. Lipparini, F. Egidi, J. Goings, B. Peng, A. Petrone, T. Henderson, D. Ranasinghe, V. G. Zakrzewski, J. Gao, N. Rega, G. Zheng, W. Liang, M. Hada, M. Ehara, K. Toyota, R. Fukuda, J. Hasegawa, M. Ishida, T. Nakajima, Y. Honda, O. Kitao, H. Nakai, T. Vreven, K. Throssell, J. A. Montgomery, Jr., J. E. Peralta, F. Ogliaro, M. J. Bearpark, J. J. Heyd, E. N. Brothers, K. N. Kudin, V. N. Staroverov, T. A. Keith, R. Kobayashi, J. Normand, K. Raghavachari, A. P. Rendell, J. C. Burant, S. S. Iyengar, J. Tomasi, M. Cossi, J. M. Millam, M. Klene, C. Adamo, R. Cammi, J. W. Ochterski, R. L. Martin, K. Morokuma, O. Farkas, J. B. Foresman and D. J. Fox, Gaussian 16, Revision C.01, Gaussian, Inc., Wallingford CT, 2016.

S2 A. D. Becke, *J. Chem. Phys.*, 1993, **98**, 5648.

S3 S. Grimme, J. Antony, S. Ehrlich and H. Krieg, *J. Chem. Phys.*, 2010, **132**, 154104.